Chapter 176
Electronic Structure Properties of *A*Te and A_2Te (*A*: Cu, Ag and Cd)

T. Premkumar, J. Mani, G. Anbalagan and R. Vidya

Abstract Efficient renewable energy generation and storage are very essential for sustainable growth on the world. New methods and materials have to be developed to convert the renewable energy into other forms of energy. This is achieved by exploring the properties of materials, which can be used in the process of energy conversion. Energy generation from waste heat using functional materials known as thermoelectric materials is receiving wide attention recently. In order to understand the properties of thermoelectric materials, we explored the electronic structure properties of *A*Te and A_2Te (*A*: Cu, Ag and Cd). Among them AgTe and CdTe are exhibiting suitable electronic properties, making them as potential thermoelectric materials.

176.1 Introduction

Chalcogenides like Cadmium Telluride have been studied for many decades for solar cell applications. Recently related phases like AgTe and CuTe are attracting wide attention for many interesting applications such as thermo-electronics and sensors. Especially Ag_2Te being a narrow band gap semiconductor is recently researched a lot owing to its wide applications on electronic, optical, magnetic and thermoelectric devices [1, 2]. The main material properties that determine thermoelectric applications are (i) low thermal conductivity (ii) high electron mobility (iii) tunable carrier concentration by doping and (iv) reversible structural transition.

In order to understand the fundamental properties of Ag_2Te and its closely related compounds, we have performed accurate first principle calculations based on Density Functional Theory (DFT) for *A*Te and A_2Te (*A*: Cu, Ag and Cd) and explored their electronic structure properties.

T. Premkumar · R. Vidya (✉)
Department of Medical Physics, Anna University, Chennai 600025, Tamil Nadu, India
e-mail: vidyar@annauniv.edu

J. Mani · G. Anbalagan
Department of Nuclear Physics, University of Madras, Chennai 600025, Tamil Nadu, India

© Springer Nature Switzerland AG 2019

R. K. Sharma and D. S. Rawal (eds.), *The Physics of Semiconductor Devices*,
Springer Proceedings in Physics 215,
https://doi.org/10.1007/978-3-319-97604-4_176

176.2 Computational Details

We have used projected augmented plane wave (PAW) method as implemented in VASP (Vienna Ab initio Simulation Package) [3]. The generalized gradient approximation (GGA) [4] was used for the exchange-correlation functional. A Monkhorst-Pack [5] k point grid was used for all our calculation. We have performed complete structural optimization by minimizing force as well as stress. The optimized structural parameters are found to be in good agreement with experimental values. We have analyzed electronic structure by calculating band features, site and orbital projected Density of States (DOS). In order to reproduce the experimental results, calculations with advanced exchange correlation functional are being carried out.

176.3 Result and Discussion

176.3.1 Electronic Structure Properties

Electronic band structure and DOS provides the fundamental electronic properties of a material. Here we have plotted the band structure of the above mentioned materials, and discussed the salient features of these compounds.

(i) CuTe and Cu_2Te

CuTe and Cu_2Te are conductors and used as a back contact material for CdTe solar cell [6] and Cu_2Te is used as a photodetectors and in photovoltaic applications [7]. CuTe has a simple orthorhombic structure described by space group *Pmmn* (No: 59) and Cu_2Te has a hexagonal Structure described by Space group P6/mmm (No: 191) were taken from the experimental results [8, 9] and optimized with force as well as stress minimization. The optimized structural parameters were used to calculate the band structure and DOS. The band structure plots of CuTe (Fig. 176.1a) and Cu_2Te (Fig. 176.1b) shows, the valence band maximum and the conduction band minimum are overlapping, and they behave like conductors.

In order to understand the nature of the overlap, we have plotted the partial as well as orbital projected DOS for CuTe and Cu_2Te. Figure 176.2 shows the total and partial DOS of CuTe (Fig. 176.2a) and Cu_2Te (Fig. 176.2b). The total DOS of CuTe spread over −10 to 10 eV energy range. The conduction band minimum having dispersed band nature, DOS also reflects the same, which leads to good conductivity. There is a peak occurs at −3 eV resulting due to the hybridization of Cu 3*d* and Te 5*p* orbitals. Band structure also shows some flat bands occurs in the same energy range, which is significance to the peak occurs in the DOS. In order to understand the hybridization of Cu 3*d* and Te 5*p* orbitals, we have plotted the orbital projected DOS for Cu 3*d* (Fig. 176.3a) and Te 5*p* (Fig. 176.3b). We can see that Cu $3d_{xy}$, $3d_{z^2}$ and Te $5p_y$ are having more occupancy compared to the other orbitals.

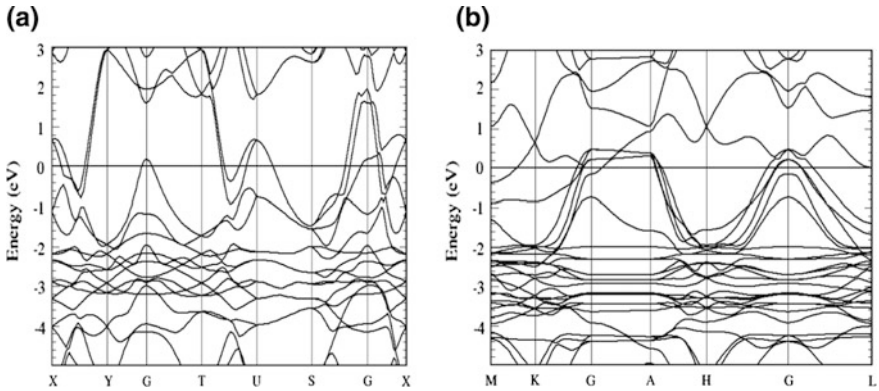

Fig. 176.1 Calculated electronic band structure of (**a**) CuTe and (**b**) Cu_2Te

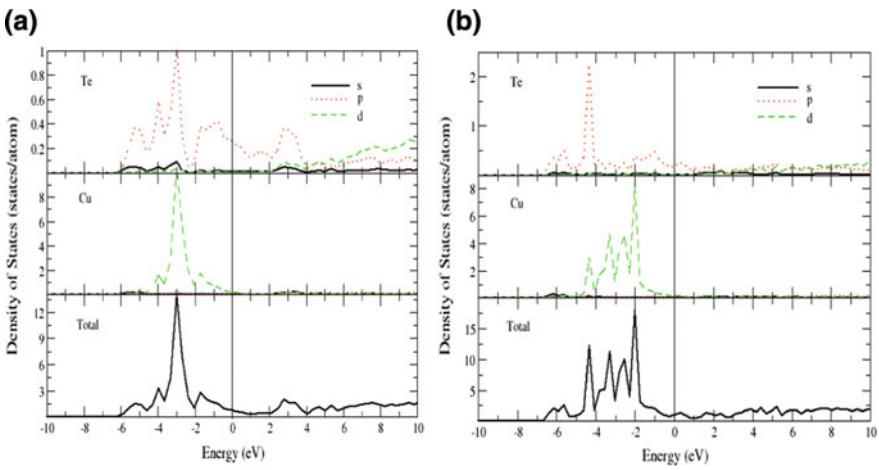

Fig. 176.2 Calculated DOS and PDOS for (**a**) CuTe and (**b**) Cu_2Te

So there is a possibility of hybridization between Cu $3d_{xy}$ and Te $5p_y$ orbitals and also Cu $3d_{z^2}$ and Te $5p_z$ orbitals. The states that crosses the fermi level are arising from p_x and p_y orbitals of Te.

The total and partial DOS of Cu_2Te (Fig. 176.2b) is spread over −10 eV to 10 eV energy range. The dispersed nature of conduction band minimum is explored by band structure as well as in the DOS proves good conductivity of the material. In the DOS, there is a peak occurs at −4.5, −3.5 and −2 eV resulting due to the hybridization of Cu 3d and Te 5p orbitals. To understand the nature of hybridization of orbitals, we have plotted the orbital projected DOS for Cu 3*d* (Fig. 176.4a) and Te 5*p* (Fig. 176.4b) orbitals. Cu $3d_{x^2-y^2}$, $3d_{z^2}$, and Te $5p_y$ orbitals having more occupancies compared to the other orbitals. So there might be possibility of

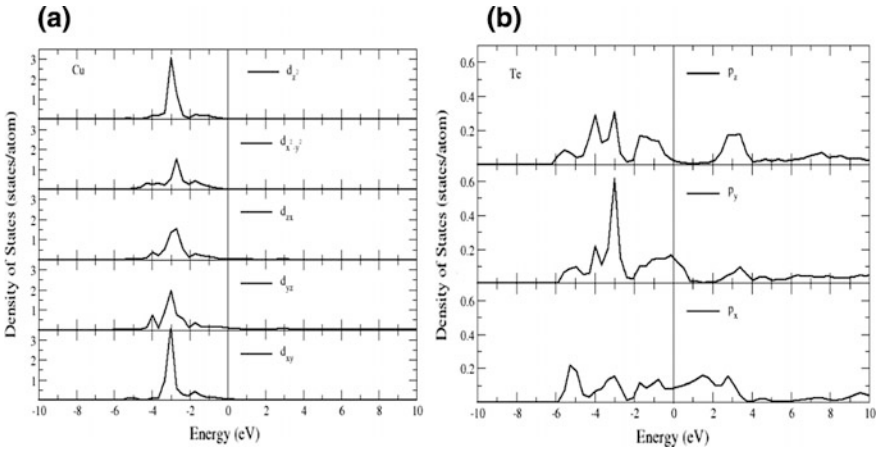

Fig. 176.3 Calculated orbital-projected DOS of (**a**) Cu *d*-orbitals and (**b**) Te *p*-orbitals in CuTe

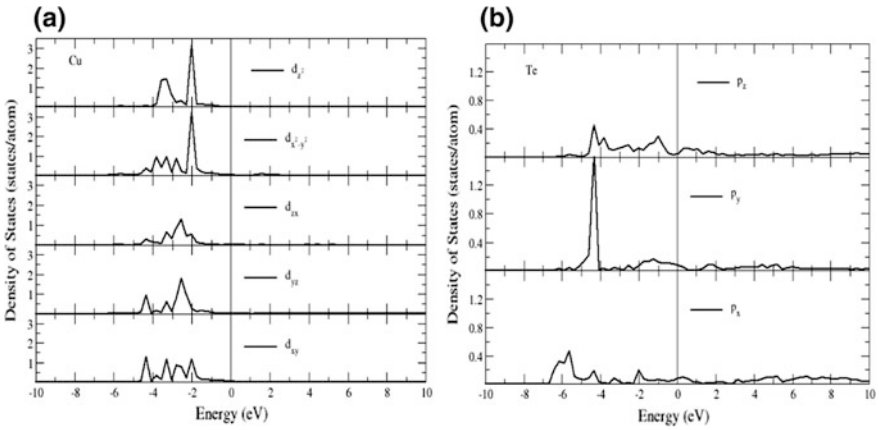

Fig. 176.4 Calculated orbital-projected DOS of (**a**) Cu *d*-orbitals and (**b**) Te *p*-orbitals in Cu_2Te

hybridization between Cu $3d_{x^2-y^2}$ and Te $5p_y$ and also Cu $3d_{z^2}$ and Te $5p_y$ orbitals. The states that crosses the fermi level are arising from p_x and p_y orbitals of Te.

(ii) AgTe

AgTe has a simple orthorhombic structure which can be described by space group *Pmnb* (No. 62). The initial parameters for structural optimization calculations were taken from the experimental values [10]. Using the optimized structural parameters after the force and stress minimization, we have plotted the band structure of AgTe (Fig. 176.5). From the band structure, it can be seen that a small band gap 0.3 eV exists between valence band maximum (VBM) and conduction band minimum

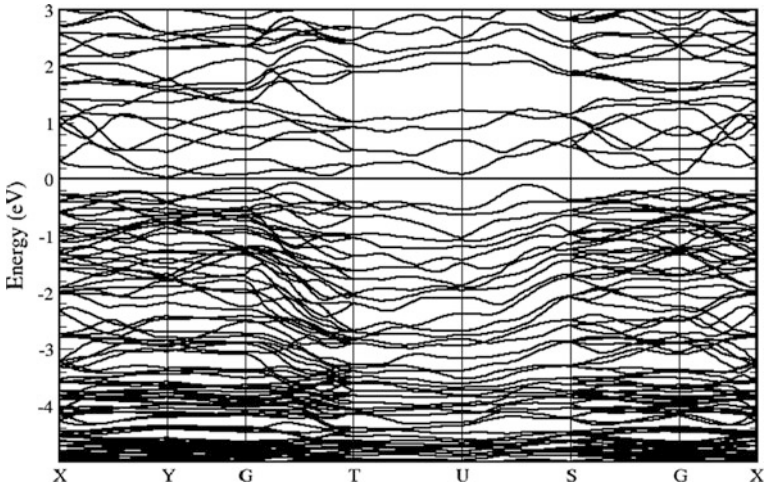

Fig. 176.5 Calculated electronic band structure of AgTe using GGA

(CBM). The top of VBM occurs between G and T and bottom of CBM occurs at Y, indicating that AgTe is an indirect band gap semiconductor. The valence band is less dispersed compare than the conduction band. So AgTe becomes n-type semiconductor if it is doped with n-type material.

(iii) Ag_2Te

Ag_2Te has a simple monoclinic structure which can be described by space group *P21/c* (No. 14). The initial parameters for structural optimization calculations were taken from the experimental values [11]. Using the optimized structural parameters after the force and stress minimization, we have plotted the band structure of Ag_2Te (Fig. 176.6).

Experimentally Ag_2Te shows a band gap of 1.72 eV [12]. However no band gap was obtained from our calculation, which is because of the inherent deficiency of DFT. We are pursuing calculations with higher advanced functionals that can reproduce the experimental results. The band structure of Ag_2Te also shows dispersed bands in valence band region as well as in conduction band region, indicating that the charge carrier conductivity will be higher if it is doped appropriately.

(iv) CdTe

CdTe is a well-known solar cell material with face centered cubic structure described by space group *F-43 m* (No. 216). The initial structural parameters were taken from experimental results [13] and optimized with force and stress minimization. The optimized structural parameters were used to plot the band structure. Our band structure (Fig. 176.7) shows direct band gap of 0.7 eV at the gamma point and contains more no of dispersed bands in the bottom of the conduction band. Top of the valence band also contains some dispersed bands as well as the flat bands. The thermal conductivity of CdTe is lesser than the electrical conductivity because of this band nature. Hence CdTe may be have good thermoelectric properties.

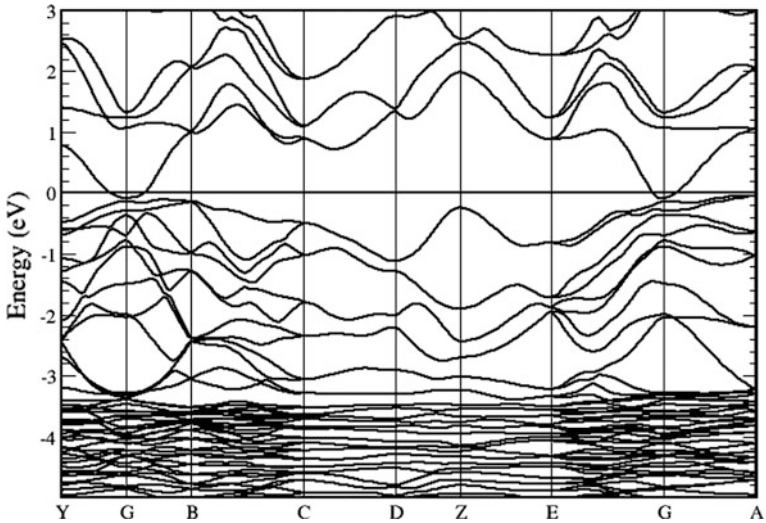

Fig. 176.6 Calculated electronic band structure of Ag_2Te using GGA

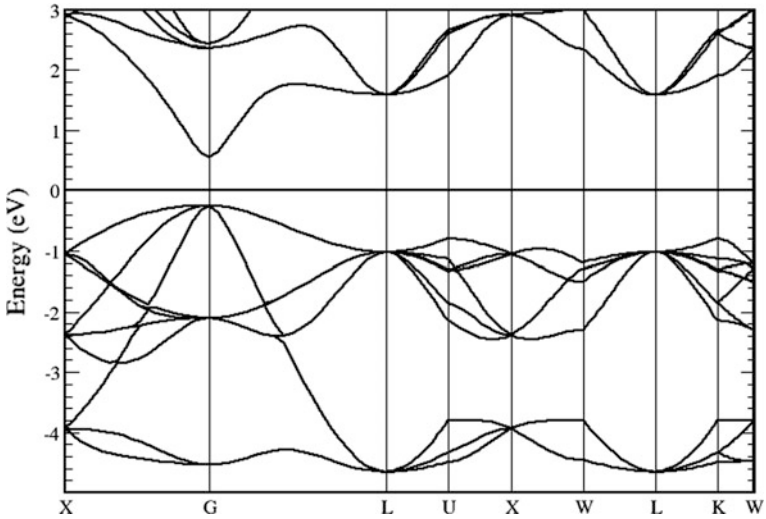

Fig. 176.7 Calculated electronic band structure of CdTe using GGA

176.4 Conclusion

The materials CuTe and Cu_2Te are having dispersed bands in their conduction band minimum. So, they are good conductors and may be used as back contact materials for solar calls, photo detectors and photo voltaic applications. CdTe shows the

direct band gap of 0.7 eV and dispersed band in the conduction band minimum leads to good electrical conductivity and because of some flat bands on the valence band maximum, the thermal conductivity is less than the electrical conductivity, which is very essential for thermoelectric applications. AgTe is having the more number of flat bands in the valence band compared than the valence band of Ag_2Te. So, AgTe having good electrical conductivity rather than the thermal conductivity. CdTe and AgTe are preferable materials to be used in the thermoelectric applications. Calculations with more advanced exchange correlation functional are being done and their thermoelectric properties are explored.

Acknowledgements The authors acknowledge Department of Science and Technology (DST) and Science and Engineering Research Board (SERB), India for providing financial support through the project SB/FTP/PS-009/2014 under the DST-Young Scientist Scheme.

References

1. M. Zhang, H. Park, J. Kim, H. Park, Chem. Mater. **27**, 5189–5197 (2015)
2. W. Zhang, R. Yu, W. Feng, Y. Yao, PRL **106**, 156808 (2011)
3. G. Kresse and J. Furthmuller, Comput. Mater. Sci. **6**, 15 (1996)
4. J. P. Perdew, S. Burke, M. Ernzarhof, Phys. Rev. Lett. **77**, 3865 (1996)
5. H. Monkhorst and J. Pack, Phys. Rev. B **13**(12), 5188 (1976)
6. Y. Zhang, B.S.J. Zhou, Z. Sun, Comput. Mater. Sci. **81**, 163–169 (2014)
7. H.M. Pathan, C.D. Lokande, Bull. Mater. Sci. **27**, 85 (2004)
8. R.V. Baranova, Z.U. Pinsker, Kristallografiya **9**, 104–106 (1964)
9. H.N. Nowotny, Metallforschung **1**, 40–42 (1946)
10. L. Bindi, P.G. Spry, C. Cipriani, Am. Miner. **89**, 1043–1047 (2004)
11. J. Schneider, H. Schuiz, Zeitschrift fuer kristallographie **203**, 1–5 (1979–2010) (1993)
12. V.B. Prabhune, V.J. Fulari, Opt. Commun. **282**, 2118–2122 (2009)
13. M. Rabadanov, I.A. Verin, Y.M. Ivanov, V.J. Simonov, Kristallografiya **46**(4), 703–709 (2001)